Hindawi Publishing Corporation
International Journal of Corrosion
Volume 2012, Article ID 185842, 7 pages
doi:10.1155/2012/185842

Research Article

Effect of Minor Alloying Elements on the Corrosion Behavior of Fe40Al in NaCl-KCl Molten Salts

G. Salinas,[1] J. G. Gonzalez-Rodriguez,[1] J. Porcayo-Calderon,[2] V. M. Salinas-Bravo,[2] and M. A. Espinoza-Medina[3]

[1] *CIICAP, Universidad Autónoma del Estado de Morelos, Avendia Universidad 1001, Colonia Chamilpa, 62209 Cuernavaca, MOR, Mexico*
[2] *IIE, Gerencia de Procesos Térmicos, Avenida Reforma 120, 62490 Temixco, MOR, Mexico*
[3] *Facultad de Ingeniera Mecanica, Universidad Michoacana de San Nicolás de Hidalgo, 58000 Morelia, MICH, Mexico*

Correspondence should be addressed to J. G. Gonzalez-Rodriguez, ggonzalez@uaem.mx

Received 2 February 2012; Accepted 18 May 2012

Academic Editor: Vesna Mišković-Stanković

The hot corrosion behavior of Fe40Al intermetallic alloyed with Ag, Cu, Li, and Ni (1–5 at.%) in NaCl-KCl (1 : 1 M) at 670°C, typical of waste gasification environments, has been evaluated by using polarization curves and weight loss techniques and compared with a 304-type stainless steel. Both gravimetric and electrochemical techniques showed that all different Fe40Al-base alloys have a much higher corrosion resistance than that for stainless steel. Among the different Fe40Al-based alloys, the corrosion rate was very similar among each other, but it was evident that the addition of Li decreased their corrosion rate whereas all the other elements increased it. Results have been explained in terms of the formation and stability of an external, protective Al_2O_3 layer.

1. Introduction

Sodium and potassium impurities present in the form of chloride or sulfates are very corrosive constituents under certain combustion conditions such as waste incinerators and biomass-fired boilers [1, 2]. Early failure of the thermal components frequently occurs due to the complex reactions between the metallic materials and the hostile combustion environment. Problems with process equipment resulting from fireside corrosion have been frequently encountered in incinerators. The major problem is the complex nature of the feed (waste) as well as corrosive impurities which form low-melting point compounds with heavy and alkali metal chlorides which prevent the formation of protective oxide scales and then causes an accelerated degradation of metallic elements [1]. In particular, under reducing conditions such as those typical of the operation of waste gasification plants or even under localized reducing conditions, which frequently arise in the case of incorrect operation of waste incineration systems, it is difficult to form protective oxide scales such as Cr_2O_3, SiO_2, and Al_2O_3 on the surface of structural materials. Thus, the corrosion attack can be further enhanced under reducing atmospheres in the presence of salt deposits [2].

The effect of individual KCl, NaCl, and their mixtures with heavy metal chlorides or sulfates on the corrosion behavior of a series of alloy systems has been studied in detail so far [2–9]. It is generally realized that Cr is not as effective element for corrosion resistance of Fe-based and Ni-based alloys due to chloride attack. In contrast, alumina-(Al_2O_3-) forming alloys exhibit promising candidate materials considering the better high temperature resistance of alumina over chromia and their properties such as lower cost, low density, high strength, and good wear resistance [10–13].

In order to obtain more information on the corrosion mechanisms taking place, electrochemical techniques are more appropriated than gravimetric methods. Since a molten salt acts as an electrolyte, electrochemical techniques such as potentiodynamic polarization curves and linear polarization resistance (LPR) measurements can be used just

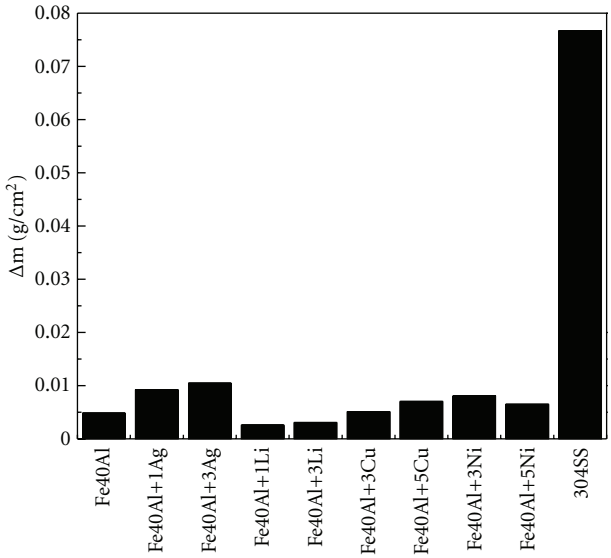

Figure 1: Effect of Ag, Li, Cu, and Ni on the weight loss for Fe40Al alloy in NaCl-KCl (1 : 1 molar ratio) deposit in static air at 670°C.

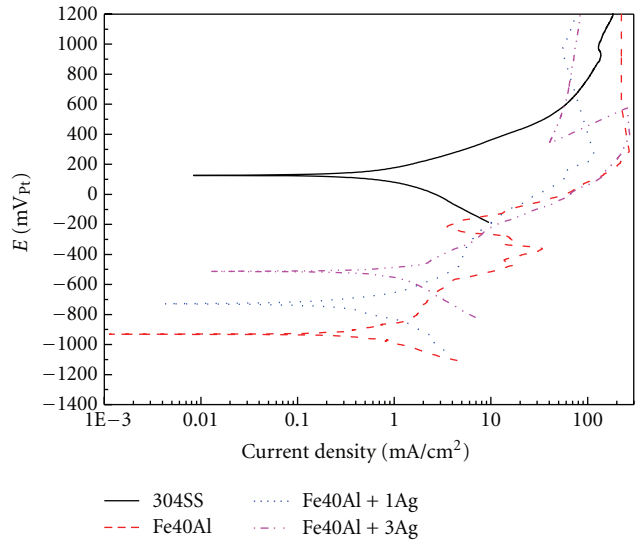

Figure 2: Effect of Ag on the polarization curve for Fe40Al alloy in NaCl-KCl (1 : 1 molar ratio) salt in static air at 670°C.

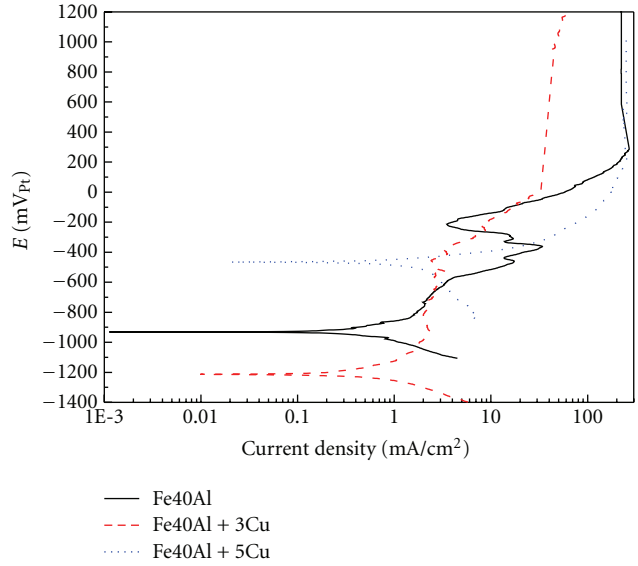

Figure 3: Effect of Cu on the polarization curve for Fe40Al alloy in NaCl-KCl (1 : 1 molar ratio) salt in static air at 670°C.

like Ducati et al. [14] showed in one of the earliest works on this topic. Zeng et al. used electrochemical impedance spectroscopy (EIS) studies for the corrosion of two-phase Cu-15Al alloy in the eutectic (Li, K)$_2CO_3$ at 650°C [15] and for Ni_3Al alloy in (Li, Na, K)$_2SO_4$ at 650°C [16]. They found that the complex plane of the electrochemical impedance suggested that the fast corrosion rate of these alloys was due to the formation of a nonprotective oxide and that the corrosion process was controlled by the diffusion of oxidants. Shirvani et al. [17] used polarization curves to study the corrosion performance of the slurry Si-modified aluminide coating on the nickel base super alloy In-738LC exposed to Na_2SO_4—20 wt.% NaCl melt at 750°C. Zhu et al. [18] used Tafel extrapolation, linear polarization resistance, chronopotentiometry, and EIS to determine corrosion rates of iron and iron-based alloys in molten carbonate melts for both cathode and anode in molten carbonate fuel cell (MCFC) environments. Cuevas-Arteaga and coworkers [19–21] have successfully used electrochemical techniques to study the corrosion of materials used in sulfate+vanadate environments and obtained information about both the type and mechanisms of corrosion on these environments. Thus, this work deals with an electrochemical study of the effect of adding alloying element such as Cu, Li, Ni, and Ag to a Fe40Al intermetallic alloy corroded in NaCl-KCl (1 : 1 M) at 670°C. For comparison, traditional weight loss experiments have been performed too.

2. Experimental Procedure

Cast ingots of binary Fe-40 at.% Al and ternary Fe40Al-X (X = 1 and 3 at.% for Cr or Li, 3 and 5 at.% for Ni or Ag) alloys were fabricated using a high-frequency vacuum induction furnace. Chemical elements of high purity (99.9%) were placed in an alumina crucible placed inside a graphite crucible in order to be induction melted under vacuum. The molten Fe-40Al, Fe40Al-X alloys were poured into a rectangular cooper mould. The produced ingots were cut by a diamond wheel cutter in small rectangular parallelepiped pieces of surface area ranging from 1.5 to 2.5 cm^2. Potentiodynamic polarization curves and weight loss measurements were used. Details of the experimental setup for the electrochemical cell used in this work are given elsewhere [22]. The body of the cell was a 15 mL silica crucible. The most important elements were a reference and auxiliary electrodes, made of a 0.5 mm diameter platinum (Pt) wire inside a mullite tube and filled with commercial refractory, ceramic cement. The amount of salt in each run was 0.5 g for an exposed area of 1.0 cm^2 under static

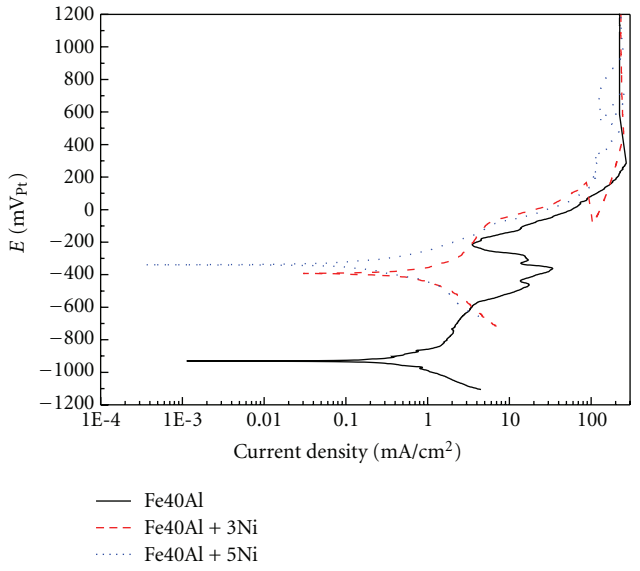

Figure 4: Effect of Ni on the polarization curve for Fe40Al alloy in NaCl-KCl (1 : 1 molar ratio) salt in static air at 670°C.

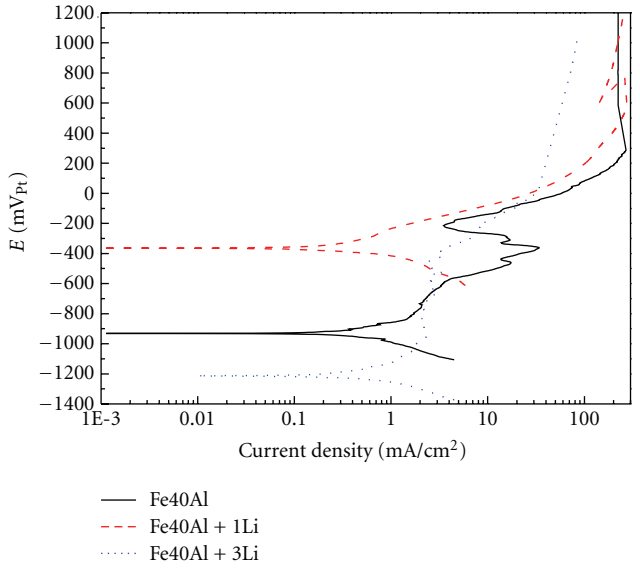

Figure 5: Effect of Li on the polarization curve for Fe40Al alloy in NaCl-KCl (1 : 1 molar ratio) salt in static air at 670°C.

conditions. The electrical contact was made by welding an 80 wt.% Cr-20 Ni wire to the specimen. Polarization curves were obtained by polarizing the specimens from −500 to +1500 mV$_{Pt}$ with respect to the free corrosion potential value, E_{corr}, at a scanning rate of 1.0 mV/s. Corrosion current density values, I_{corr}, were calculated by using the Tafel extrapolation method, which is valid for the sweep rates used here according to [21] and taking an extrapolation zone of ±250 mV around the E_{corr} value once it was stable. The working salt consisted of 500 mg/cm^2 of an eutectic mixture of NaCl-KCl, 1 : 1 M, analytical grade for each test. The testing temperature was 670°C in static air condition.

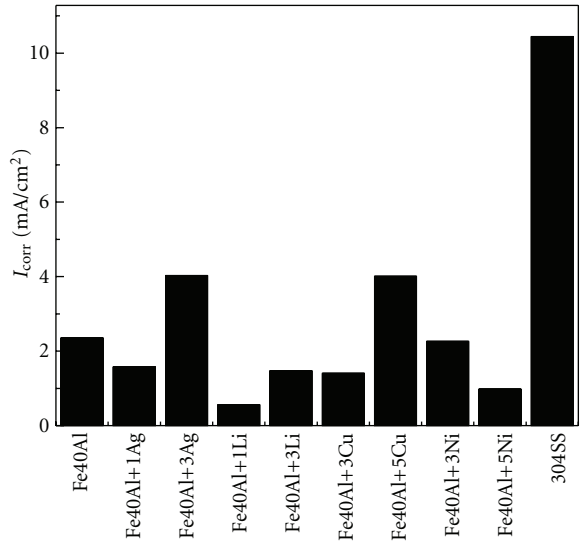

Figure 6: Effect of Ag, Li, Cu, and Ni on the I_{corr} values for Fe40Al alloy in NaCl-KCl (1 : 1 molar ratio) deposit in static air at 670°C.

Prior the tests, the specimen surfaces were prepared by the standard technique of grinding with SiC from 240 to 600 grit emery paper, washed with water, and degreased with acetone. Weight loss tests were carried out in electric furnaces in a static air during 100 hours. All materials were machined into specimens with dimensions of about 10 mm × 15 mm × 1.5 mm, then grounded to 600 grade emery paper, and cleaned in a supersonic bath of acetone. After the corrosion tests, the corrosion rate was measured as weight loss. Three specimens of each condition test were decaled and chemically cleaned according to ASTM G1 81 standard. For comparison, the same tests were done with a 304-type stainless steel. One of each heat was mounted in bakelite in cross-section and polished to analyze the subsurface corrosive attack using a scanning electron microscopy (SEM) aided with energy dispersive spectroscopy (EDX) to carry out microchemical analysis.

3. Results and Discussion

Figure 1 shows that the mass loss for the different alloys alters being exposed to an eutectic NaCl-KCl mixture at 670°C during 100 hours. It can be seen that 304-type stainless steel suffered the greatest corrosion rate, more than one order of magnitude higher than that for all the Fe40-based alloys. Li et al. [2] obtained very similar results with an Fe45Al alloy in NaCl-KCl mixture at 670°C during 100 hours. Among the different Fe40Al-based alloys, the addition of either 1 or 3% Li decreased the corrosion rate of unalloyed Fe40Al alloy, whereas the addition of Ag, Ag or Ni increased it; however, this difference is marginal.

The effect of 1 and 3% Ag on the polarization curves for Fe40Ag base alloy, together with that one for 304-type stainless steel, is shown on Figure 2. It can be seen that unalloyed Fe40Al-based alloy displays an active-passive behavior, with an E_{corr} value close to −927 mV and an I_{corr}

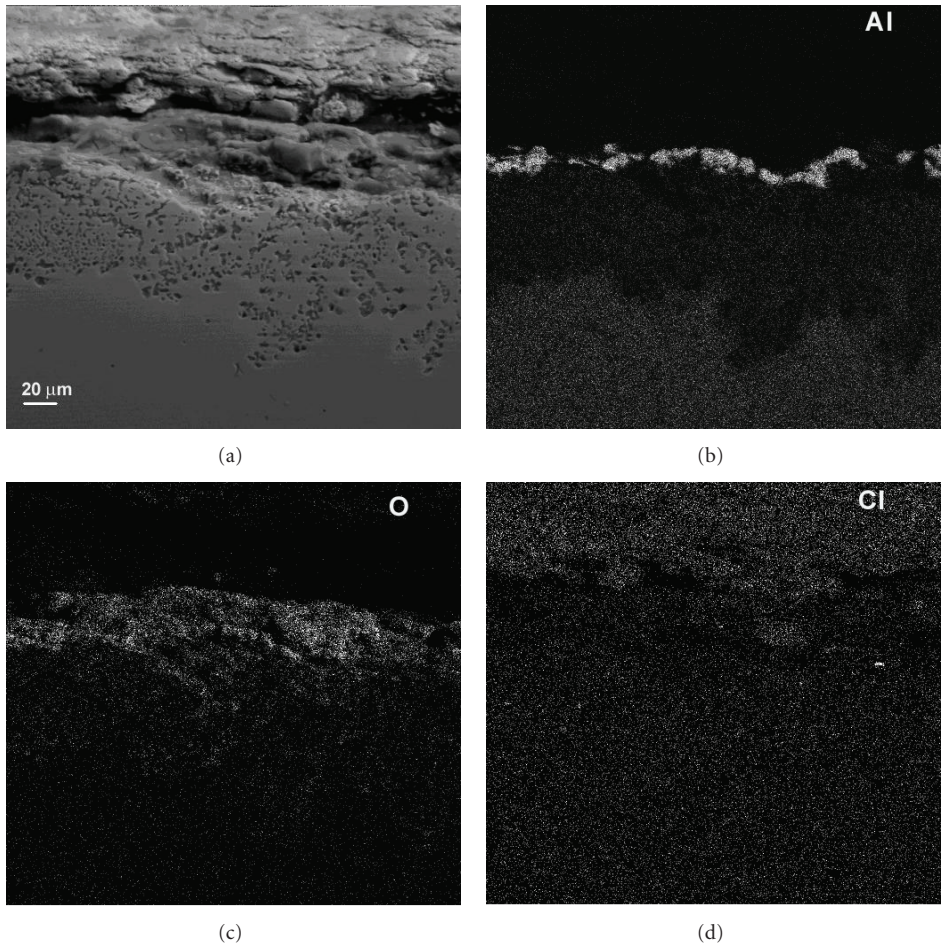

Figure 7: Micrograph of Fe40Al alloy corroded in NaCl-KCl at 670°C together with the X-ray mappings of Al, O, and Cl.

value of 0.15 mA/cm^2. As the applied potential is more anodic, the anodic current density value increases until it reaches a more or less constant value, that is, a passive region, between −800 and −600 mV, where a sudden increase in the current density value appears. Some anodic peaks are observed at −500 and −400 mV, respectively. A second, narrow passive region can be observed around −200 mV, after which the anodic current density increases once again until it reaches an anodic limit current density. This might be due to the presence of an external layer which acts as a barrier against the ingress of the aggressive species. When Ag was added into the alloy, the E_{corr} value is made more anodic and the I_{corr} value is increased. The presence of a passive region in the Ag-containing alloys is not very clear; however, for both alloys, around −450 mV the anodic current density value showed a more or less constant value, although this was not so evident for the alloy containing 3% Ag. The presence of an anodic limit current density, lower than that observed for the Fe40Al base alloy, is observed in both cases at a potential value close to 200 mV. The corrosion current density value for 304-type stainless steel was higher than that for the three Fe40Al-based alloys for at least one order of magnitude, and there was no evidence of a passive region. According to the mass loss data (Figure 1) 304-type stainless steel had the highest corrosion rate too.

The addition of 3% Cu did not affect very much the I_{corr} value as the addition of 5% Cu did, as can be seen on Figure 3. The free corrosion potential became more active with the addition of 3% Cu, but it became much nobler when 5% Cu was added. The passive region in the alloy containing 3% Cu was much wider and more stable than that shown by the unalloyed base alloy, starting around −1100 mV and finishing around −300 mV, where a breakdown potential is obtained. There was no evidence of apassive region for the alloy containing 5% Cu, only anodic dissolution, with the highest anodic current density value. Similarly, the addition of either 3 or 5% Ni shifted the E_{corr} value towards the noble direction, whereas the I_{corr} value was slightly decreased only with the addition of 5% Ni (Figure 4). The presence of a passive region was found only with the addition of 3% Ni between −300 and 0 mV, where the breakdown potential was reached. After this point, an anodic limit current density value is observed in both cases, with a value slightly lower than that found for unalloyed Fe40Al-base alloy.

Finally, when Li was added (Figure 5), the E_{corr} value became nobler with the addition of 1% but more active with

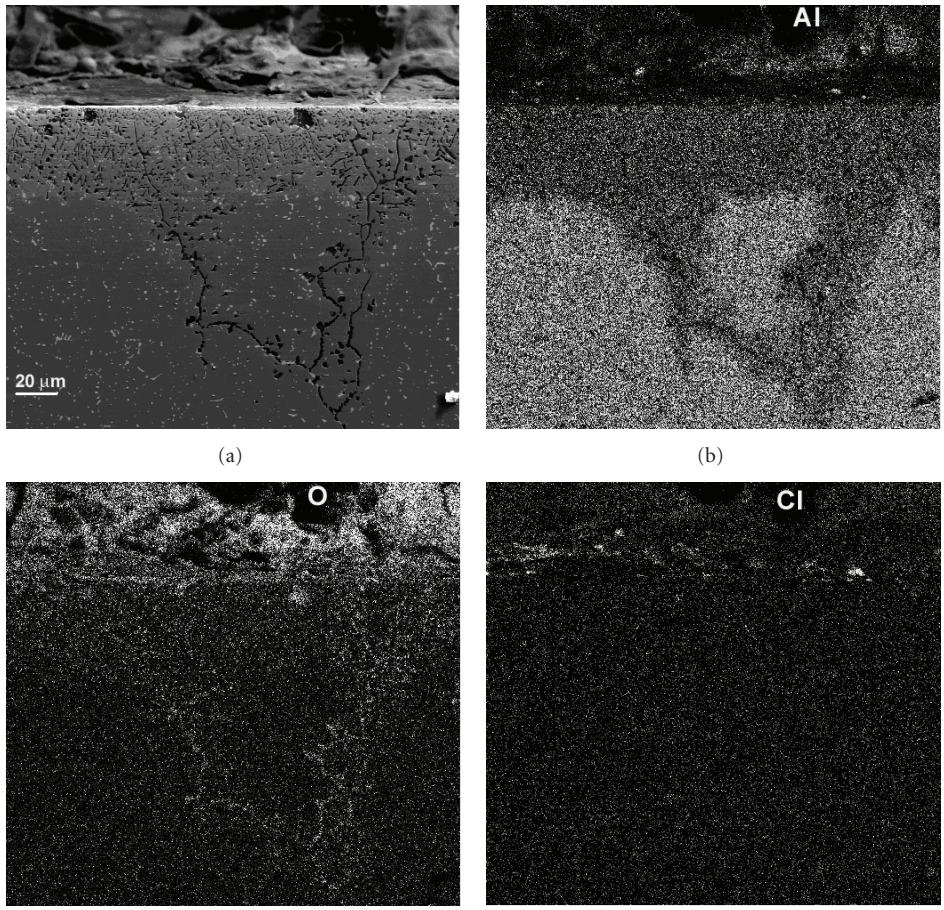

Figure 8: Micrograph of Fe40Al + 3Ag alloy corroded in NaCl-KCl at 670°C together with the X-ray mappings of Al, O, and Cl.

3% Li. In addition, the corrosion rate, expressed in terms of the corrosion current density values, was decreased in both cases, just as evidenced by the weight loss results in Figure 1. A much wider and stable passive region than that found on the unalloyed Fe40Al based-alloy is found between −1000 and −300 mV. Unlike this, no passive region can be seen with the addition of 1% Li, but only anodic dissolution until an anodic limit current density is reached. Thus, it can be seen that different alloying elements have a different effect on the electrochemical behavior of Fe40Al alloy in molten NaCl-KCl. Table 1 gives a summary of the different electrochemical parameters obtained from the polarization curves. Figure 6 gives the corrosion current density values, I_{corr}, for all the Fe40Al-based alloys, where it can be seen that the highest value corresponds to the 304-type stainless steel, whereas the lowest value corresponds to the Li-containing alloys. Similar results were obtained with the weight loss test (Figure 1), thus, both gravimetric and electrochemical techniques gave similar results: all the different Fe40Al-based alloys have a better corrosion performance than that for 304-type stainless steel in the NaCl-KCl mixture at 670°C.

Figure 7 shows a micrograph of corroded unalloyed Fe40Al-based alloy together with the X-ray mappings of Al, O, and Cl, where it can be seen the presence of both Al and O, maybe representing the formation of what seems to be a protective Al_2O_3 oxide, which is the responsible for the passive behavior observed in the polarization curve for this alloy (Figure 2); the absence of Al and O in some points indicates that the external Al_2O_3 oxide is porous and it has been dissolved by aggressive molten salt. Li et al. [2], corroding an Fe45Al alloy in NaCl-KCl salt at

Table 1: Electrochemical parameters obtained from polarization curves.

Alloy	β_a (mV/dec)	β_c (mV/dec)	I_{corr} (mA/cm^2)	E_{corr} (mV)
FeAl-base	311	223	1.5	−927
FeAl-1Ag	293	398	2.3	−730
FeAl-3Ag	269	432	4.0	−510
FeAl-1Li	159	65	0.5	−363
FeAl-3Li	346	134	1.4	−1212
FeAl-3Cu	169	180	1.4	−1212
FeAl-5Cu	78	191	4	−460
FeAl-3Ni	159	207	2.2	−395
FeAl-5Ni	177	222	0.9	−340
304SS	243	311	10.4	125

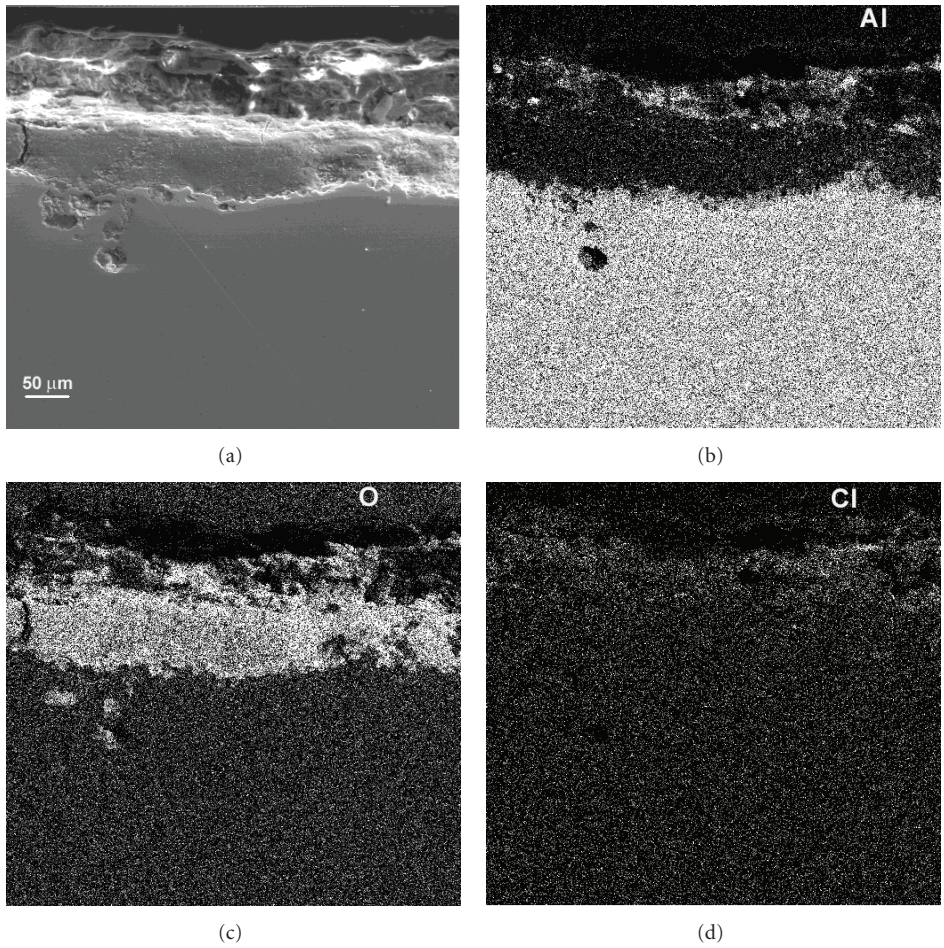

Figure 9: Micrograph of Fe40Al + 3Li alloy corroded in NaCl-KCl at 670°C together with the X-ray mappings of Al, O, and Cl.

670°C during 48 hours, found Al_2O_3 as the main compound formed on the external layer. For the alloy containing 3 Ag, Figure 8, there is evidence of Al, O, and Cl, indicating the formation of an external protective Al_2O_3 oxide dissolved by the Cl-containing salt; however, there is evidence of internal oxidation along the grain boundaries. The formation of an external Al_2O_3 oxide is more evident for the alloy containing 3Li (Figure 9), where it can be seen that aggressive ions such as Cl^- practically remain outside the protective Al_2O_3 oxide, but, eventually, the molten salt dissolves this oxide and dissolves the underlying alloy. Both chlorine and aluminum seem to form a compound on the external salt, which, according to Li et al. [2], could be liquid $AlCl_3$, which melts at 192°C. An Al-depleted and an O-rich zone can be observed in all alloys. These two alloys showed an active-passive behavior in their polarization curves (Figures 2 and 5), which is due to the presence of a very adherent, protective Al_2O_3 layer.

Thus, it can be seen that the corrosion protection of an alloy against salt melt attack depends on the chemical stability of both the kind of metal and their compounds such as oxides and chlorides. In fact, a breakdown of the protective oxide readily occurs by dissolution into the melt, and the degradation rate can be especially fast if the oxide has a high solubility in the melt. Since from a thermodynamic point of view, Al is the most reactive element among all the different investigated elements here; Al chloride or oxide forms preferentially over the other elements. At the melt-substrate interface, the oxygen potential is low while the chlorine potential is relatively high, and, consequently, liquid aluminum chloride forms there and transports outwards, leaving an aluminum depleted layer as observed in Figures 7–9. Near the melt-atmosphere interface,the transition from aluminum chloride to its oxide occurs, which onlyrelatively low oxygen pressure is needed because of the very stablenature of aluminum oxide. Therefore, the preferential removal of aluminum from the matrix is enhanced, basically in the form of highly volatile liquid chloride. This process seems to be beneficial to help establish a protective alumina, Al_2O_3, scale due to a fast aluminum supply. The role of the different alloying elements is to help to make more stable the alumina layer on top of the alloy and increase the alloy corrosion rate in the melt.

4. Conclusions

A study of the effect of alloying elements such as Ag, Li, Cu, and Ni on the corrosion resistance of Fe40Al intermetallic

alloy beneath a NaCl-KCl mixture in air at 670°C has been carried out by using both weight loss and potentiodynamic polarization curves. Both techniques have shown that the corrosion rate of the different Fe40Al-based alloys is much lower than that for 304-type stainless steel for nearly one order of magnitude. Addition of Li decreased the corrosion rate of unalloyed Fe40Al-base alloy, whereas the addition of Ag, Ni, or Cu increased it. However, the corrosion rate for the different Fe40Al-based alloys was within the same order of magnitude. Results have been explained in terms of the formation and stability of an external, protective alumina, Al_2O_3, layer.

References

[1] C. S. Ni, L. Y. Lu, C. L. Zeng, and Y. Niu, "Electrochemical impedance studies of the initial-stage corrosion of 310S stainless steel beneath thin film of molten $(0.62Li,0.38K)_2CO_3$ at 650°C," *Corrosion Science*, vol. 53, no. 3, pp. 1018–1024, 2011.

[2] Y. S. Li, M. Spiegel, and S. Shimada, "Corrosion behaviour of various model alloys with NaCl-KCl coating," *Materials Chemistry and Physics*, vol. 93, no. 1, pp. 217–223, 2005.

[3] Nobuo Otsuka, "Effects of fuel impurities on the fireside corrosion of boiler tubes in advanced power generating systems—a thermodynamic calculation of deposit chemistry," *Corrosion Science*, vol. 44, no. 2, pp. 265–283, 2002.

[4] Y. Shinata and Y. Nishi, "NaCl-induced accelerated oxidation of chromium," *Oxidation of Metals*, vol. 26, no. 3-4, pp. 201–212, 1986.

[5] N. Hiramatsu, Y. Uematsu, T. Tanaka, and M. Kinugasa, "Effects of alloying elements on NaCl-induced hot corrosion of stainless steels," *Materials Science and Engineering A*, vol. 120-121, no. 1, pp. 319–328, 1989.

[6] Y. S. Li, M. Sanchez-Pasten, and M. Spiegel, "High temperature interaction of pure Cr with KCl," *Materials Science Forum*, vol. 461-464, pp. 1047–1054, 2004.

[7] F. Wang and Y. Shu, "Influence of Cr content on the corrosion of Fe-Cr alloys: the synergistic effect of NaCl and water vapor," *Oxidation of Metals*, vol. 59, no. 3-4, pp. 201–214, 2003.

[8] C. J. Wang and Y. C. Chang, "NaCl-induced hot corrosion of Fe-Mn-Al-C alloys," *Materials Chemistry and Physics*, vol. 76, no. 2, pp. 151–161, 2002.

[9] Y. S. Li, Y. Niu, and W. T. Wu, "Accelerated corrosion of pure Fe, Ni, Cr and several Fe-based alloys induced by $ZnCl_2$–KCl at 450°C in oxidizing environment," *Materials Science and Engineering A*, vol. 345, no. 3, pp. 964–970, 2003.

[10] F. H. Stott and G. C. Wood, "Internal oxidation," *Materials Science and Technology*, vol. 4, no. 12, pp. 1072–1078, 1988.

[11] G. Han and W. D. Cho, "High-temperature corrosion of Fe_3Al in 1% Cl_2Ar," *Oxidation of Metals*, vol. 58, no. 3-4, pp. 391–413, 2002.

[12] F. Lang and Z. Yu, "Corrosion behavior of Fe–40Al sheet in N_2–$11.2O_2$–$7.5CO_2$atmospheres with various SO_2 contents at 1273 K," *Intermetallics*, vol. 11, no. 2, pp. 135–141, 2003.

[13] Y. Kawahara, "High temperature corrosion mechanisms and effect of alloying elements for materials used in waste incineration environment," *Corrosion Science*, vol. 44, no. 2, pp. 223–232, 2002.

[14] U. Ducati, G. L. Coccia, and G. Caironi, "Electrochemical evaluation of hot corrosion resistance of metallic materials," *Materials Chemistry and Physics*, vol. 8, no. 2, pp. 135–145, 1983.

[15] C. L. Zeng, P. Y. Guo, and W. T. Wu, "Electrochemical impedance spectra for the corrosion of two-phase Cu-15Al alloy in eutectic $(Li, K)_2CO_3$ at 650°C in air," *Electrochimica Acta*, vol. 49, no. 9-10, pp. 1445–1450, 2004.

[16] C. L. Zeng, W. Wang, and W. T. Wu, "Electrochemical impedance models for molten salt corrosion," *Corrosion Science*, vol. 43, no. 4, pp. 787–801, 2001.

[17] K. Shirvani, M. Saremi, A. Nishikata, and T. Tsuru, "Electrochemical study on hot corrosion of Si-modified aluminide coated In–738LC in Na_2SO_4–20 wt.% NaCl melt at 750°C," *Corrosion Science*, vol. 45, no. 5, pp. 1011–1021, 2003.

[18] B. Zhu, G. Lindbergh, and D. Simonsson, "Electrochemical impedance studies of the initial-stage corrosion of 310 S stainless steel beneath thin film of molten $(0.62Li, 0.38K)_2CO_3$ at 650°C," *Corrosion Science*, vol. 41, no. 9, pp. 1497–1513, 1999.

[19] C. Cuevas-Arteaga, J. Uruchurtu-Chavarín, J. Porcayo-Calderon, G. Izquierdo-Montalvo, and J. Gonzalez, "Study of molten salt corrosion of HK–40 m alloy applying linear polarization resistance. And conventional weight loss techniques," *Corrosion Science*, vol. 46, no. 11, pp. 2663–2679, 2004.

[20] C. Cuevas-Arteaga, J. Uruchurtu-Chavarín, J. G. González, G. Izquierdo-Montalvo, J. Porcayo-Calderón, and U. Cano, "Corrosion evaluation of Alloy 800 in sulfate/vanadate molten salts," *Corrosion*, vol. 60, no. 4, pp. 520–527, 2004.

[21] C. Cuevas-Arteaga, "Corrosion study of HK–40 m alloy exposed to molten sulfate/vanadate mixtures using the electrochemical noise technique," *Corrosion Science*, vol. 50, no. 3, pp. 650–663, 2008.

[22] J. G. Gonzalez-Rodriguez, O. L. Arenas, J. Porcayo-Calderon, V. M. Salinas-Bravo, M. Casales, and A. Martinez-Villafañe, "An electrochemical study of the effect of B on the corrosion of atomized Fe40Al intermetallics in molten Na_2SO_4," *High Temperature Materials and Processes*, vol. 25, no. 2, pp. 293–301, 2006.